WEAK AND STRONG COUPLING BETWEEN THE *elsA* CFD SOLVER AND THE HOST HELICOPTER COMPREHENSIVE ANALYSIS

P. Beaumier, M. Costes, B. Rodriguez, M. Poinot, B. Cantaloube
ONERA, Châtillon, France

Abstract

Two techniques aiming at solving the fluid-structure coupling problem for a helicopter rotor in forward flight are described and compared in this article. The first one is the weak coupling, where the fluid mechanics and the aerodynamics problems are coupled in an iterative and not time accurate manner. The second one is the strong coupling, which is time accurate since exchanges between the fluid mechanics and the aerodynamics solvers are done at each time step. Comparisons of the results obtained by the two coupling methods are done for a test case of the 7A 4-bladed rotor in high speed forward flight: a 3D RANS solver is used as aerodynamic model and a comprehensive code with beam model for the structure problem. For this stabilized periodic problem, it is shown that the two coupling methods provide almost identical results. Attempts to improve the correlation between calculations and experiment are finally presented.

Introduction

The helicopter is characterized by its rotating lifting surfaces, and more especially the main rotor which provides both the lift and the propulsive forces to the rotorcraft. This specific aspect induces an increased aerodynamic complexity which has a large impact on the whole architecture of the helicopter. Indeed, the combination of forward speed and rotation introduces a dissymmetry in the blade velocity relatively to the ambient air, which creates significant 1/rev fluctuating loads at the source of vibrations, and more importantly of large periodic fluctuating hinge moments which require to be minimized in order to avoid the mechanical breaking of the rotor head. The articulated hub and/or the introduction of soft elements at the root of the blades (hingeless, bearingless rotors) is the technical way to solve this problem, but it naturally introduces a strong interaction between the blade aerodynamics and its motion and deformation. Indeed, for a given blade pitch control input, the blade flapping and lead-lag angles, as well as the blade deformation (more especially in torsion), result from the balance between the aerodynamic, the inertial and the elastic forces and moments applied to the rotor, which are inter-dependent. This balance also determines the global forces and moments which the main rotor provides to the complete helicopter, which also has an influence on the rotor motion.

For computing the helicopter aerodynamics, it is therefore necessary to solve the fluid-structure coupling problem for each desired flight configuration, the blades motion and deformation being an unknown of the problem. This coupling is generally done by helicopter comprehensive analyses, using simplified aerodynamic models in order to render the problem easier to solve. As a matter of fact, the degrees of freedom of the blade dynamics can thus explicitly appear in the aerodynamic formulation, so that the full coupled system is represented by a system of differential equations which can be solved by cheap and standard numerical procedures. When performing a CFD rotor computation, the blades motion and deformation are prescribed as a boundary condition obtained from the comprehensive analysis. Nevertheless, whatever the simplified aerodynamic model is in the comprehensive analysis, the aerodynamic loads and moments computed by CFD are significantly different from those of the simplified model, because the aerodynamics of the rotor is complex, with large unsteady, compressibility, three-dimensional, interactional and viscous effects. As a result, the CFD solution is not consistent with the rotor motion and deformation. The only way to get consistent aerodynamic results between comprehensive analysis and CFD is to couple these two methods until globally converged fluid and structure solutions are reached.

The work presented in this paper was completed in the frame of the French-German CHANCE project, which aimed at the simulation of the complete helicopter with CFD, and combined the effort of ONERA, DLR, IAG, Eurocopter and Eurocopter Deutschland [1]. In this context, a coupling methodology between CFD rotor solutions and blade dynamics computed by comprehensive analysis was developed. Two types of coupling have been considered, the weak and the strong coupling techniques, following the methodologies described in [2]. The objective of the paper is to describe these

two coupling procedures, underlying their similarities and differences. Examples of applications of the coupling are presented for both types of coupling, using the 7A rotor database. Attempts to improve the strong coupling results are then proposed before drawing some conclusions.

Numerical methods

CFD method

The CFD code used at ONERA in CHANCE is *elsA* [3]. The development of this object-oriented software for aerodynamics was initiated by ONERA in 1997. This multi-application CFD software solves the Reynolds-Averaged Navier-Stokes equations for all the aerospace configurations from the low subsonic regime to hypersonic, including fixed wing, rotary wing, turbomachinery, space launcher and missile configurations. It uses a cell-centered finite volume discretization for multi-block meshes, including overset and patched grid capabilities. It has a wide range of numerical techniques available for space and time resolution, as well as for turbulence modeling. In the present work a 2nd order centered discretization in space with Jameson's artificial viscosity was used. For the resolution in time, the dual time-stepping method or the Gear implicit sub-iterative method was used in order to converge towards the 2nd order-accurate solution. These techniques allow the use of large azimuthal steps: $\Delta\psi$=1.2deg for the present simulations. For turbulence modelling, the low cost algebraic model of Michel is used for the applications presented in this paper.

Rotor comprehensive analysis

The helicopter dynamics code used in CHANCE is the HOST code from Eurocopter [4]. This method has the capability to compute the aeromechanics and flight dynamics of the complete helicopter or of its isolated components (main rotor, tail rotor). The blade dynamics is described by beam theory with modal decomposition in order to reduce the number of unknowns. For the blade aerodynamics, it uses a simplified model based on blade element theory with 2D airfoil tables. Several induced velocity models are available, from simple analytic ones (such as the Meijer-Drees model), vortex wake models (METAR prescribed wake and MESIR free wake), and dynamic inflow models (such as the Pitt-Peters model). Additionally, a set of corrections are available which aim at improving the accuracy of the 2D quasi-steady airfoil model (unsteadiness, Reynolds number effects, dynamic stall).

For computing the rotor, two different methodologies can be used in HOST. The trim solution, valid for steady flight conditions of the helicopter, makes the assumption that the flow is periodic in time at the frequency of the rotation speed of the rotor multiplied by the number of blades, so that all rotor parameters can be decomposed into Fourier series in order to reduce the number of unknowns. The rotor solution is then obtained for user-prescribed trim conditions, such as rotor lift and propulsive forces, zero first harmonic components of the flapping angles. The other approach works in the time domain and is adapted from flight dynamics problems. Starting from a trimmed solution, the fluid-structure problem is solved in a time-marching approach for prescribed rotor control angles, the degrees of freedom being the rotor flap and lead-lag motions as well as the blade deformation in torsion, flap and lead-lag.

Coupling methodologies

As indicated above, two different coupling methodologies have been developed in CHANCE, called the weak coupling and the strong coupling. They were developed in common by the various partners of CHANCE, under the main responsibility of IAG (University of Stuttgart) for strong coupling and of ONERA and DLR for weak coupling [5], [6].
The weak coupling technique follows the HOST trim procedure (Figure 1). A periodic solution is assumed, which allows exchanging data between HOST and *elsA*, rotor revolution per rotor revolution. The HOST fluid-structure coupling process uses the simplified aerodynamic forces of HOST F_{2D}^{n} corrected by the difference between the *elsA* results F_{3D}^{n-1} and those coming from the simplified aerodynamic model of the previous rotor revolution F_{2D}^{n-1}. The main advantage of this coupling is that it provides a trimmed solution of the rotor consistent with the 3D aerodynamic loads and moments coming from the CFD. The drawback of this approach is that the fluid-structure coupling does not use the CFD results directly at each step of the HOST computation and therefore all the damping properties of the fluid come from the simplified aerodynamic model, which might be inaccurate.
Contrary to that, the strong coupling technique [2] uses the time-marching algorithm of HOST (Figure 2), and the three components of aerodynamic forces and moments W_n are computed by the CFD at each time step, and used by HOST to integrate the Lagrange's equation in order to compute the blade motion Q_n, velocity and deformation for the next time step of the aerodynamic solution.

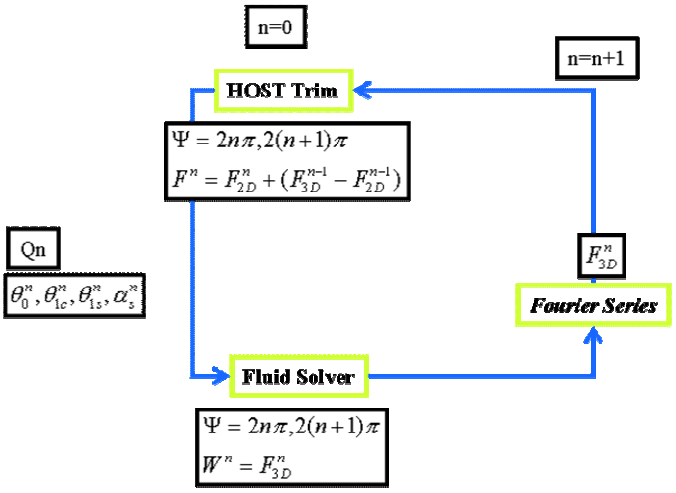

Figure 1: Schematic of the weak coupling

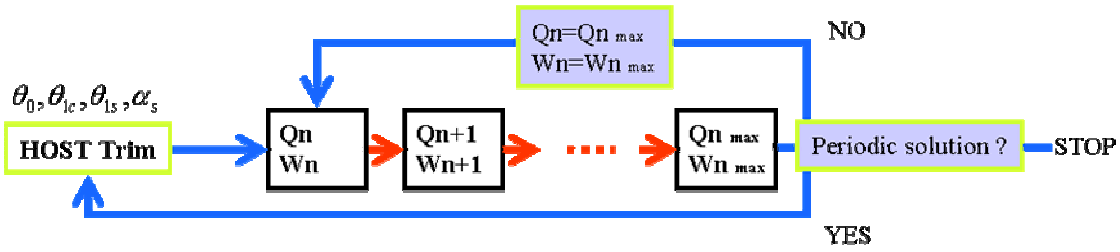

Figure 2: Schematic of the strong coupling

This kind of coupling can thus be made time-consistent since the dynamic response of the blade is obtained with the CFD aerodynamics and no additional simplified model is required. For steady flight conditions of the helicopter, where the flow field around the rotor blade is periodic, the coupling is pursued until a periodic aerodynamic solution is obtained for the rotor blades. The main drawback of the approach is that, since the rotor control angles are prescribed during such a procedure, the solution obtained at convergence is not trimmed. An external trim has thus to be performed in order to modify the rotor control angles. The idea of the method is to linearize the relationship between the control angles and the trim conditions by evaluating an approximate Jacobian matrix [*J*] (using the 2D simple aerodynamic model of HOST):

$$\begin{bmatrix} \theta_0 \\ \alpha_q \\ \theta_{1C} \\ \theta_{1S} \end{bmatrix}_{new} = \begin{bmatrix} \theta_0 \\ \alpha_q \\ \theta_{1C} \\ \theta_{1S} \end{bmatrix}_{old} + [J] \cdot \left(\begin{bmatrix} ZB \\ XB \\ \beta_{1S} \\ \beta_{1C} + \theta_{1S} \end{bmatrix}_{new} - \begin{bmatrix} ZB \\ XB \\ \beta_{1S} \\ \beta_{1C} + \theta_{1S} \end{bmatrix}_{old} \right)$$

In other terms, at the end of the coupling scheme, new controls are estimated, knowing the present vector (ZB, XB, β_{1S}, $\beta_{1C}+\theta_{1S})_{old}$ and the vector to be obtained (defined by the trimmed conditions). Once the controls are updated, a new aerodynamic integration is done up to a periodic solution. If this new solution is not trimmed, the procedure is repeated. The method is approximate and presently not automatic.

Exchange of data between HOST and *elsA*

An important aspect of the coupling concerns the software part which allows exchanging the data between HOST and *elsA*. For both weak and strong coupling, the approach adopted is fully modular, the exchange interfaces with *elsA* being written in Python language. The modular and interpreted software architecture provides a high-flexibility for extracting and processing the data. There is no need to integrate specific processing in the kernel of the CFD solver. Since the comprehensive analysis and the CFD parts of the solution require different levels of computing capabilities, the two methods are run on different computers which communicate via the Python interface. In the weak coupling approach, the communication is performed by exchanging files

between *elsA* and HOST, which is understandable since the exchange of data is performed rotor revolution per rotor revolution, which represents a time scale of the order of one to five hours for the exchange frequency. This is no more the case for the strong coupling where the exchange of data happens at each physical time step of the computation. The exchange of data is thus performed via memory and also through a TCP/IP interface designed by IAG, which also specifies the structure of the data to be exchanged. Nevertheless, in both cases, the data format follows the CGNS data structure [8], allowing to deal with self-consistent information easy to manipulate and readable by all CGNS-compliant softwares.

The CGNS data structures gather a large part of the context needed during the exchange between solvers. The data structure is built and transferred by means of memory-based systems and this physical representation of data increases the run-time efficiency of the whole simulation. The logical representation is CGNS compliant; it lays on the public standard and is required for all software parts included in the simulation. The solvers have to produce and use CGNS compliant data for both input and output. Such a CGNS component [9] makes our simulation software architecture open to the CFD tools, and provides a better platform for solvers or tools extension or change.

Applications

Test case: the 7A rotor

The applications are taken from the 7A rotor database, tested in the S1MA wind tunnel (ONERA, France, 1991: Figure 3). This rotor is equipped with four blades with linear aerodynamic twist (-8.3deg/R) and an aspect ratio equal to 15. The rotor diameter is 4.2m. The conditions of the high speed test case considered in the applications below are defined by:

Advance ratio, μ	0.4
Tip rotational Mach number, $M_{\Omega R}$	0.646
Non dimensional rotor lift coefficient, ZB=200.Ct/σ	12.5
Non dimensional propulsive force coefficient, XB	1.6

Table 1: trim conditions for the selected test case

The rotor trim is done to match the so-called "Modane" flapping law defined by the two equations:

- $\beta_{1S}=0$,
- $\beta_{1C}+\theta_{1S}=0$.

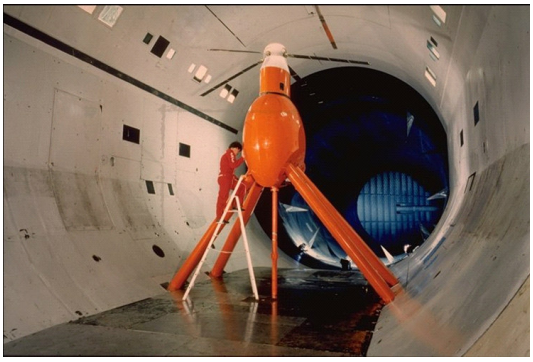

Figure 3: 7A rotor in S1MA wind tunnel

Coupled results for the isolated rotor

Grids

Multi-block grids (one C-H block per blade) are used for the simulation of the isolated rotor (Figure 4). Each block includes 189 nodes along the chord direction, 57 nodes in the spanwise direction (with 32 aerodynamic sections) and 49 nodes in the direction normal to the blade, resulting in a total number of nodes for the complete rotor approximately equal to $2.1.10^6$. At the interfaces between the 4 blocks, no interpolation is necessary because the nodes are perfectly coincident.

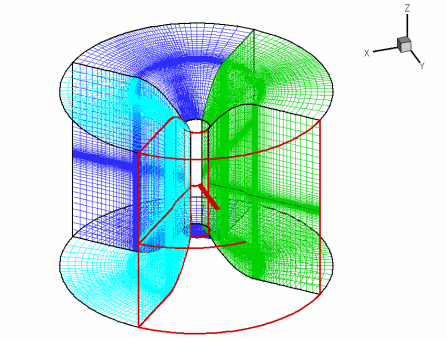

Figure 4: Multi-block grid used for RANS simulations of the isolated 7A rotor

Weak coupling

Following the conclusions drawn in [5], the coupling variables exchanged after each rotor revolution are the 3 components of the forces and the pitching moment around the blade quarter-chord line.

The convergence of the coupling process is quite fast: three iterations are sufficient to obtain a good stabilization of the control angles (collective pitch θ_0, cyclic pitch angles θ_{1C} and θ_{1S}, rotor shaft angle α_q), as illustrated in Figure 5. The good convergence can also be appreciated on the torsion response near the

blade tip, which is almost identical between iterations 2 and 3 (Figure 6).

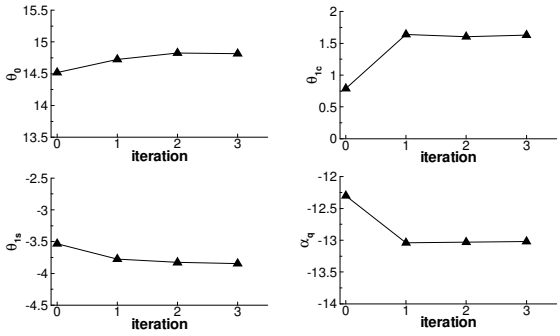

Figure 5: Convergence of the control angles during the weak coupling iterations

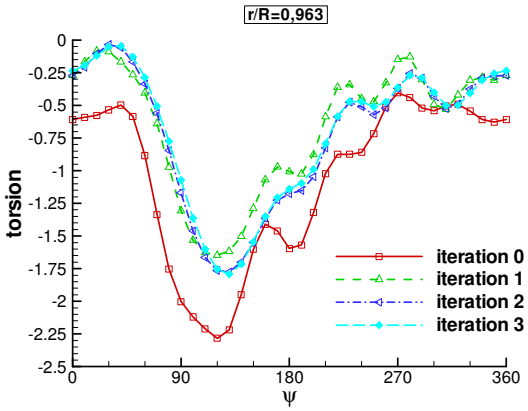

Figure 6: Evolution of tip torsion response during the weak coupling iterations

Strong coupling

Reaching the convergence for the strong coupling is more difficult than for the weak coupling. The first step is to obtain a periodic response of the blade with prescribed control angles, before adjusting them to match the correct trim. This generally requires several rotor revolutions, as already mentioned in [2] with an inviscid CFD solver. One of the difficulties is the almost non damped lead-lag motion, which made the convergence of the lead-lag degree of freedom very slow in [2]. In order to speed-up the convergence, an attempt has been made in the present study to start the first rotor revolutions with a very high damping of the lead-lag damper, and then to progressively reduce this parameter until its nominal value during the next rotor revolutions. This procedure appears to be efficient, as shown in Figure 7, where both the flapping (BETA-RP) and lead-lag (DELTA-RP) angles at the hinge are almost periodic after 9 rotor revolutions. Note that one rotor revolution represents a time interval Δt=0.06s (X axis in Figure 7). The evolution of the rotor lift coefficient ZB is also periodic and very close to its nominal value 12.5, thanks to the adjustment of the rotor control angles done after the 3rd and the 5th rotor revolution (t=0.18s and 0.3s respectively). However, the periodicity of the solution is not perfect, since there is still a reduction of the amplitude of the oscillations of the power consumed by the rotor after the 9 rotor revolutions (Figure 9).

The final solution matches the expected trim conditions quite well with the following mean values (averaged over the last rotor revolution):

- ZB=12.519 (instead of 12.5),
- XB=1.592 (instead of 1.6),
- β_{1S}=0.016 (instead of 0),
- $\beta_{1C}+\theta_{1S}$=-0.009 (instead of 0).

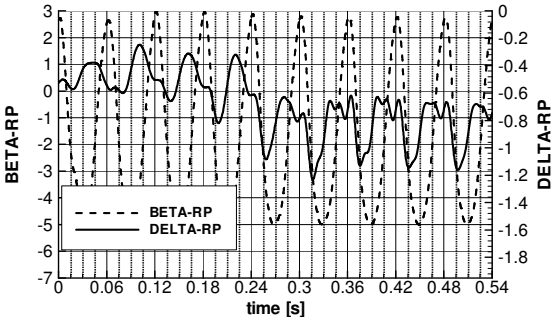

Figure 7: Convergence of the hinge flapping and lead-lag angles

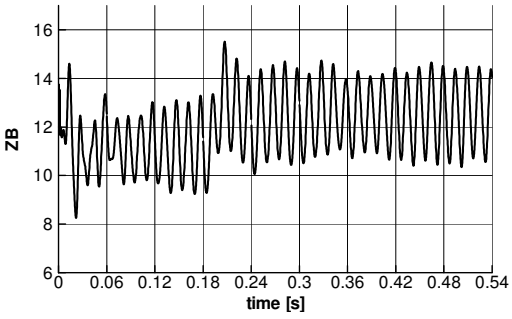

Figure 8: Convergence of the rotor lift coefficient

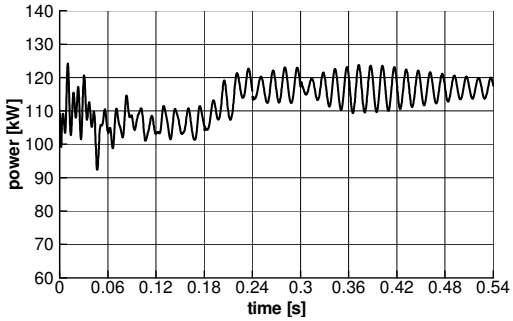

Figure 9: Convergence of the rotor power

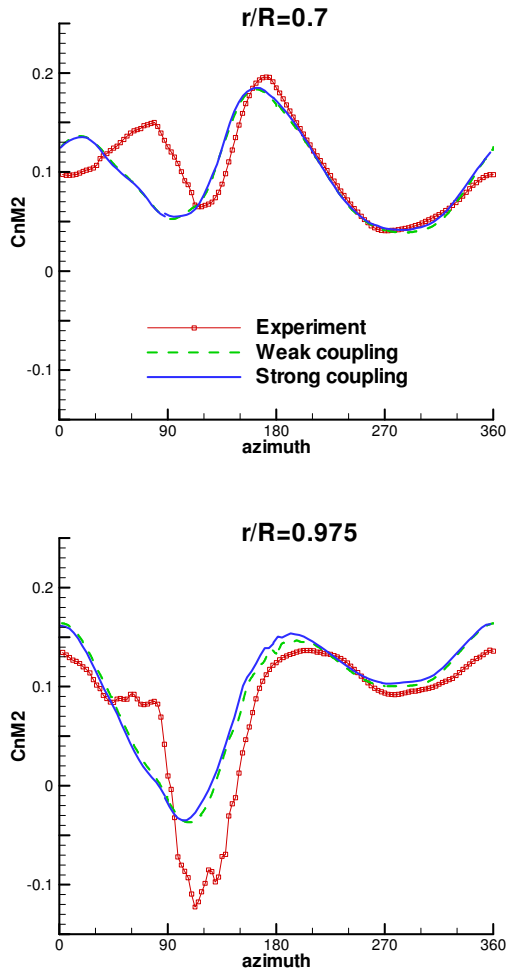

Figure 10: Airloads distribution: comparison between weak and strong coupling

Comparison between weak and strong coupling

Since both the weak and strong coupling results converge to the same flight conditions, it makes sense to compare the two solutions.

The sectional loads represented by the CnM2 coefficients at two selected spanwise locations r/R=0.7 and 0.975 are plotted in . The weak and strong coupling calculations provide very similar results, with only a very small phase shift for the most outboard section. In any case, the strong coupling does not help in improving the correlation with experiment: the prediction of the amplitude and phase of the peak of negative loading remains poor in both calculations.

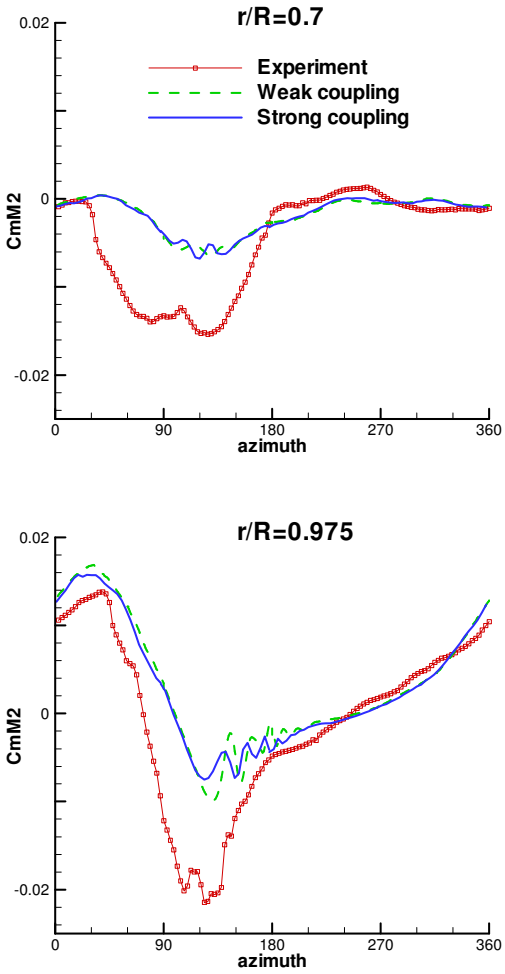

Figure 11: Pitching moment distribution: comparison between weak and strong coupling

For the sectional pitching moments (Figure 11), the two predictions are very similar too. The only small difference can be seen on the high frequency oscillations near the blade tip for the azimuth angles between ψ=120° and 180° which are slightly more damped in the strong coupling approach than in the

weak coupling approach. Here again, the strong coupling results are not really in better agreement with experiment than the weak coupling results. For the section at r/R=0.7, the predicted pitching moments remain not negative enough between ψ=0° and 180°. For the section at r/R=0.975, the highly negative pitching moments in the second quadrant (between ψ=90° and 180°) are not reached by the predictions.

It is also interesting to look at the torsion response of the blade (Figure 12). Only small differences between the weak and strong coupling results can be observed. The torsion response obtained with the weak coupling seems to have a richer harmonic content than with the strong coupling. However, this does not significantly improve the correlation with experiment. Both predictions suffer from a lack of 5/rev content resulting in low peak-to-peak amplitude of the torsion response. Note also that the elastic torsion angles are not negative enough on the advancing side (between ψ=120° and 170°): this has to be related with the poor estimation of the amplitude of the negative airloads mentioned above.

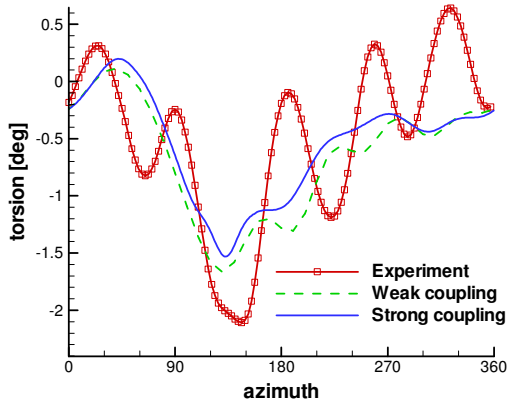

Figure 12: Torsion response: comparison between weak and strong coupling

Table 2 summarizes the values of the control angles obtained by the two coupling methods compared to experiment. Once again, this confirms that the two coupling strategies converge to similar solutions, although not identical. Furthermore, one can notice that the main discrepancy with experiment concerns the longitudinal pitch angle θ_{1C}, which is largely under-predicted by the calculations (by more than 2 degrees). This is known to be a consequence of the influence of the large test rig on which the 7A rotor was mounted. Weak coupling results accounting for this test rig have shown significant improvement in the prediction of the angle θ_{1C}, however with only minor improvement in the prediction of the phase of the peak of negative loading [7].

	θ_0	θ_{1C}	θ_{1S}	α_q
Experiment	14.54	3.43	-3.70	-13.75
Weak coupling	14.87	1.35	-3.78	-13.17
Strong coupling	14.76	1.09	-3.90	-12.75

Table 2: control angles [deg]

Globally speaking, one can conclude that the two coupling strategies provide very similar results. This conclusion was already reached in [2], when the Euler equations were solved: this remains true when solving the RANS equations. In terms of computational efficiency, the advantage is obviously for the weak coupling method, which converges 3 times faster than the strong coupling.

Attempts to improve the quality of the comparisons between CFD simulations and experiment are proposed in the following part of this paper.

Improvement of results

Influence of the accuracy of the time integration scheme

The time integration scheme used for all CFD calculations presented above was the Dual Time Stepping (DTS), used without multigrid acceleration. The convergence of the sub-iterations is controlled by a maximum number a sub-iterations and by a mean residual that has to be reached. The smaller this mean residual is, the better the convergence, but the higher the number of sub-iterations may be, and consequently the CPU time.

Recent investigations (see [7] for example) with the *elsA* solver have shown that the Gear implicit method (a Newton like technique) was more efficient for the convergence of the sub-iterations in terms of CPU time than the DTS technique. In order to investigate if a better convergence in the time integration process has an influence on the quality of the results, the strong coupling calculation of the preceding paragraph was re-started using the Gear technique. The same physical azimuthal step $\Delta\psi$=1.2deg is used. After 4 additional rotor revolutions, a new solution is obtained. This new solution is close to the trimmed solution (Table 3), thanks to another slight modification of the control angles.

	ZB	XB	β_{1S} [deg]	$\beta_{1C}+\theta_{1S}$ [deg]
Experiment	12.5	1.6	0	0
Strong coupling, DTS	12.519	1.592	0.016	-0.009
Strong coupling, Gear	12.398	1.588	-0.028	-0.048

Table 3: Trim conditions after strong coupling calculations with DTS and Gear

The influence of the improved accuracy of the time integration with the Gear technique is negligible on the sectional lift distribution CnM2 (top of Figure 13), but is significant on the pitching moment distribution especially near the blade tip (middle of Figure 13): the agreement with experiment becomes quite good in the first quadrant (from ψ=0° to 90°), and the negative pitching moment coefficients are better predicted in the second quadrant, even if they remain not negative enough compared to experiment.

As a consequence of this modification of the aerodynamic excitation, the amplitude of the torsion response is increased (bottom of Figure 13): the negative torsion deformations on the advancing side are in better agreement with experiment, but a phase shift remains. Additionally, a higher frequency component is starting to appear in the Gear results, which was largely damped in the DTS results. These encouraging results indicate that there is a need of a very accurate time integration technique in order to have a good capture of the pitching moment aerodynamic excitation.

Attempts to lower the residuals threshold in the sub-iterations or to reduce the physical time step did not show additional improvements. The poor prediction of the peak of negative loading near the blade tip remains unexplained. However, it can be expected that improvements in the pitching moments response may improve the torsion response (especially the phase) and finally have consequences of the aerodynamic incidences and lift.

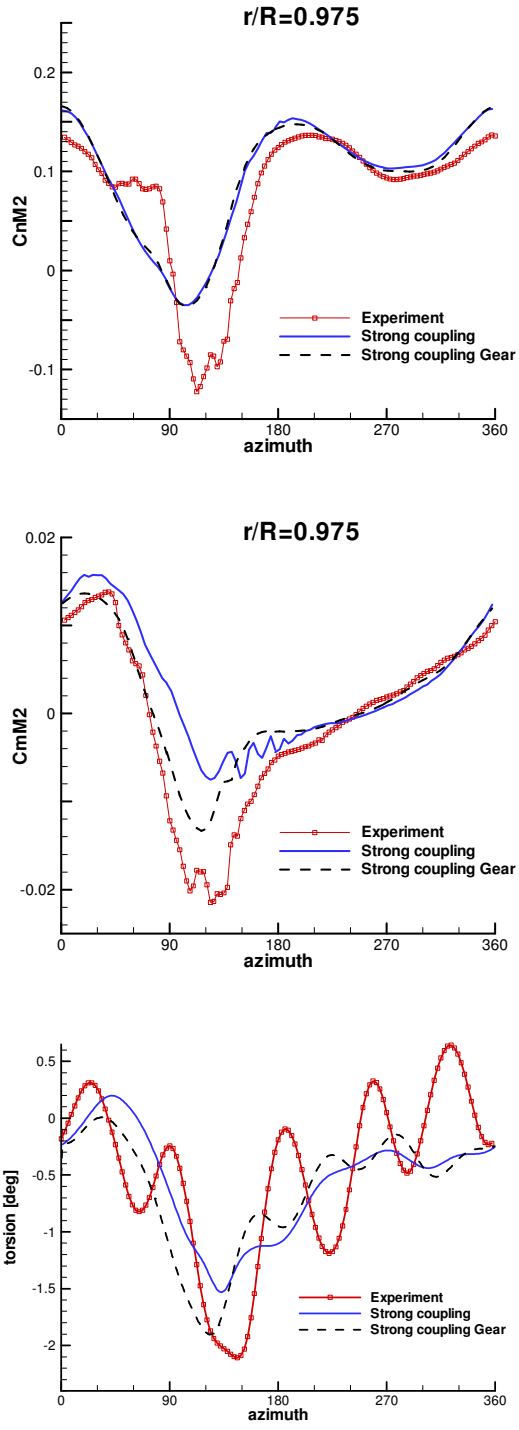

Figure 13: Influence of time integration method in the CFD solver on the results of the strong coupling

Strong coupling with measured control angles

One of the deficiencies in the strong coupling calculations presented up to now is the fact that the test rig is not accounted for. As already explained, it was shown in that the test rig has an influence on the longitudinal pitch angle θ_{1C}. This can result in a better prediction of the phase of the negative CnM2 peak near the blade tip. One way to investigate the influence of the θ_{1C} angle on the airloads response is to perform a strong coupling calculation with measured control angles θ_0, θ_{1C}, θ_{1S} and α_q. This is different from performing a strong coupling calculation without trimming the rotor, since the strong coupling calculations presented above were initialized by a trimmed solution obtained by the comprehensive code HOST.

	ZB	XB	β_{1S} [deg]	$\beta_{1C}+\theta_{1S}$ [deg]
Experiment	12.5	1.6	0	0
Strong coupling, exp. control angles	10.023	1.269	-2.6	-0.769

Table 4: Trim conditions for a strong coupling calculation with experimental control angles

A periodic solution is obtained after 9 rotor revolutions (using the Gear time integration technique). Of course, when prescribing the experimental control angles, the final CFD solution has no reason to be close to the test case in terms of rotor global forces. Indeed, the rotor lift and propulsive force coefficients ZB and XB are quite low compared to experiment and the trim conditions in terms of flapping angles are not respected (Table 4).

Although the CFD solution is not trimmed, it is interesting to see the difference with the strong coupling results without prescribing the control angles. Figure 14 presents a selection of this comparison for the most outboard section r/R=0.975. Surprisingly, only small differences are observed, mainly on the lift response (top of Figure 14) in the first, third and fourth quadrants. But the phase and amplitude of the peak of negative loading are almost unchanged. Similarly, the pitching moment and torsion response (middle and bottom of Figure 14) are very comparable. Such a result is surprising considering the fact that the phase of the airloads response should be modified, since the control angles (especially the θ_{1C} pitch angle) is significantly different. In fact, it seems that the flapping motion of the blade is modified in such a way that the aerodynamic incidences are not changed significantly.

The final prediction in terms of airloads or pitching moment distribution is not really improved with prescribed experimental control angles.

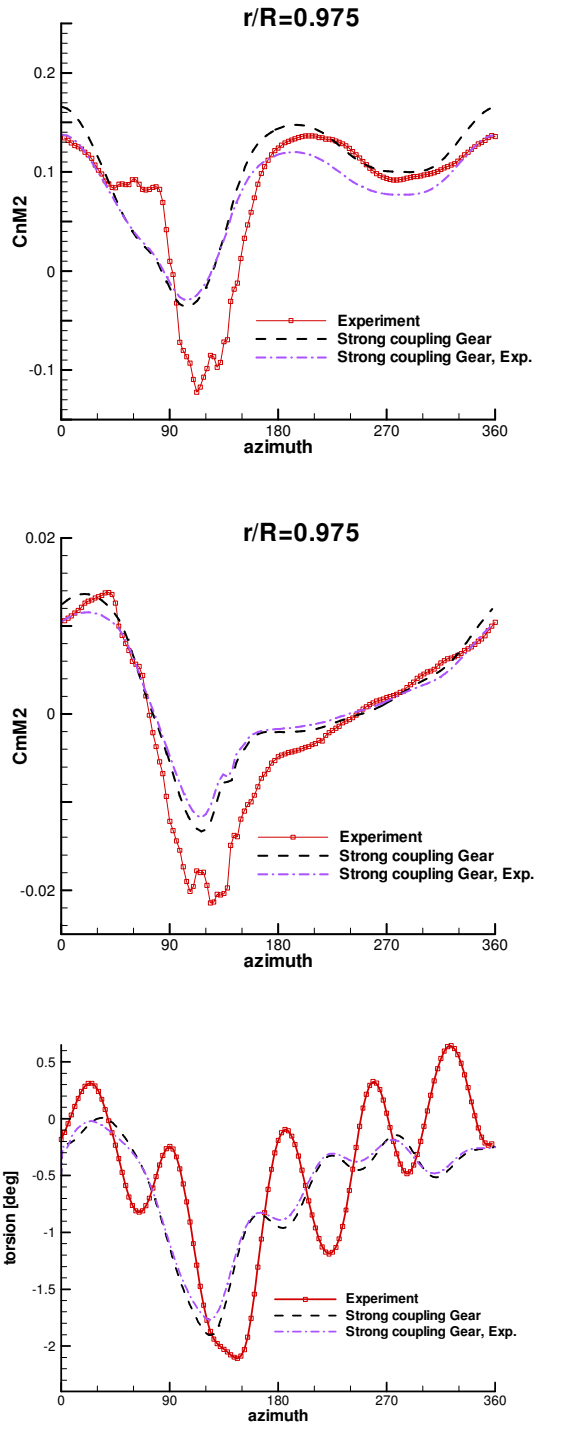

Figure 14: Influence of experimental control angles on the results of the strong coupling

Concluding remarks

Two methodologies to couple a 3D aerodynamics solver and a comprehensive rotorcraft analysis have been described and applied to an isolated rotor. The first one (weak coupling) is an iterative method, not time accurate, which automatically provides a trimmed solution. The second one (strong coupling) is time accurate, but requires additional effort to obtain a trimmed solution. Both methods couple the HOST comprehensive code where an elastic beam model is used and the *elsA* code solving the RANS equations.

On the test case of the 7A rotor in high speed forward flight, it has been shown that:

- the convergence of the strong coupling towards a periodic solution is slower than for the weak coupling; one of the reasons is the lead-lag motion, which is not damped (an artificial damping has been used in order to speed-up the convergence); the other one comes from the necessity to adjust the control angles in order to perform the rotor trim;
- a strong coupling calculation requires about 3 times more computational effort than a weak coupling calculation;
- using the same numerical parameters and grids in both cases, the weak and strong coupling approaches provide very similar results in terms of sectional lift and pitching moments distributions, elastic torsion response and rotor trim;
- the strong coupling approach does not improve the correlation with experiment.

This very last disappointing result does not mean that there is no interest in the strong coupling. Indeed, the method is much more general than the weak coupling, and can be used for the simulation of non stabilized or non periodic flights, which is not the case for the weak coupling.

The sensitivity of the CFD viscous solution with respect to the accuracy of the time integration scheme has been evaluated, through a comparison between the Dual Time Stepping and the Gear integration methods. The pitching moments and the elastic torsion predictions are in better agreement with experiment when the most accurate method (Gear) is used. However, the prediction of the peak of negative loading on the advancing side near the blade tip remains poorly predicted. The influence of grid density on this parameter should be investigated in order to improve the quality of the predictions.

From the view point of coupling methodologies, future work will concern the harmonization of the weak and strong coupling strategies, so that strong coupling calculations ensuring the correct rotor trim can be done in a more efficient way.

Acknowledgments

The authors would like to acknowledge the SPAé from the French DGA (Délégation Générale de l'Armement) and the DPAC for their financial support all along the CHANCE program.

References

[1] M. Costes, K. Pahlke, A. d'Alascio, C. Castellin, A. Altmikus, *Overview of results obtained during the 6-year French-German CHANCE project*, AHS 61st Annual Forum, Grapevine, June 1-3, 2005

[2] A.R.M. Altmikus, S. Wagner, P. Beaumier, G. Servera, A *comparison: weak versus strong modular coupling for trimmed aeroelastic rotor simulations,* AHS 58th Annual Forum, Montreal, June 11-13, 2002

[3] L. Cambier, M. Gazaix, *"elsA: an efficient object oriented solution to CFD complexity",* 40th AIAA Aerospace Science Meeting and Exhibit, Reno NV, January 14-17, 2002

[4] B. Benoit, A-M. Dequin, K. Kampa, W. Grunhagen, P-M. Basset, B. Gimonet, *HOST, A general helicopter simulation toll for Germany and France*, Ahs 56th Annual Forum, Virginia Beach, May 2000

[5] G. Servera, P. Beaumier, M. Costes, *A weak coupling method between the dynamics code HOST and the 3D unsteady code WAVES*, 26th European Rotorcraft Forum, The Hague, Sept. 2000

[6] K. Pahlke, B. van der Wall, *Calculation of multi-blade rotors in high speed forward flight with weak fluid-structure coupling*, 27th European Rotorcraft Forum, Moscow, Sept. 2001

[7] B. Rodriguez, C. Benoit, P. Gardarein, *Unsteady computations of the flowfield around a helicopter rotor with model support*, 43rd AIAA Aerospace Sciences Meeting and Exhibit, Reno (USA), Jan. 2005

[8] D.M.A Poirier, D.R. Allmaras, D.R. McCarthy, M.F. Smith, F.Y. Enomoto, *"The CGNS System"*, AIAA Paper 98-3007

[9] M. Poinot, M. Costes, B. Cantaloube, *Application of CGNS software components for helicopter blade fluid-structure strong coupling*, 31st European Rotorcraft Forum, Firenze, Sept.2005